ACS APPLIED ELECTRONIC MATERIALS

pubs.acs.org/acsaelm Review

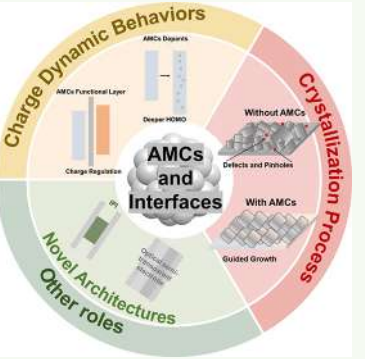
The Interfacial Regulation Strategies of Perovskite Light-Emitting Diodes through Alkali Metal Compounds

Yongjian Chen, Xiankan Zeng, Wen Li,* and Weiqing Yang*

Cite This: ACS Appl. Electron. Mater. 2026, 8, 1456−1465 Read Online

ACCESS | Metrics & More | Article Recommendations

ABSTRACT: Perovskite light-emitting diodes exhibit great potential in the fields of display and lighting, yet their performance is still limited by interfacial nonradiative recombination and charge imbalance. Although alkali metal compounds (AMCs) have been extensively studied as perovskite lattice components or bulk dopants, the strategy of using AMCs as functional interlayers or interfacial modifiers has received far less attention than it deserves. Despite the fact that this strategy has been proven effective, there is still a lack of systematic sorting and review of its multidimensional action mechanisms. We aim to fill this gap and explore the multiple interfacial roles of AMCs. This review not only provides a perspective for understanding the interfacial physicochemical processes related to AMCs, but also offers theoretical insights for the design and fabrication of high-performance and stable device.



KEYWORDS: *Perovskite, light-emitting diodes, alkali metal compounds, interlayer, charge imbalance*

1. INTRODUCTION

Metal halide perovskite materials have triggered a revolutionary transformation in the field of optoelectronics. The external quantum efficiency (EQE) of perovskite light-emitting diodes (PeLEDs) has surged from less than 1% to over 30%,[1,2] demonstrating immense application potential. However, the stability of PeLEDs with "sandwich-like" multilayer structures still lags behind the theoretically predicted values, with interfacial nonradiative recombination and charge imbalance significantly undermining device durability.[3−6]

The performance of PeLEDs depends not only on the quality of the emissive layer (EML) itself but also, to a greater extent, on the interfaces between functional layers,[7−9] which serve as hubs for charge injection, transport, and recombination, while simultaneously being active regions for defect accumulation, ion migration, and nonradiative recombination.[10,11] Therefore, interface engineering is regarded as the key to addressing the performance bottlenecks of PeLEDs. Among various interface modification materials, alkali metal compounds (e.g., CsF, K_2SO_4, LiF, CsCl) have emerged as a simple, efficient, and multifunctional research focus. Initially, AMCs were widely used as electron injection layers (EIL) in organic light-emitting diodes (OLED).[12,13] Drawing on this experience, researchers introduced them into PeLEDs and soon found that their roles extend far beyond improving electron injection. AMCs play multiple synergistic roles at interfaces of PeLEDs, with their influences spanning the entire chain from film preparation to device physics.

AMCs can serve as effective lattice components or dopants for perovskite materials (AX, where A represents Li, Na, K, Rb, Cs, and X represents F, Cl, Br, I), which has been extensively studied and discussed.[14,15] Therefore, this review aims to provide a unique and comprehensive review and summary of the interface regulation effects of AMCs in PeLEDs. We will mainly conduct discussions around two core roles including regulation of charge dynamic behaviors and crystallization processe. By integrating these multidimensional action mechanisms, this review will clarify how AMCs act as a "versatile agent" to synergistically enhance the overall performance of PeLEDs from both physical and chemical perspectives. Finally, based on current understanding, we will point out the key scientific issues and technical challenges, and propose prospects for future research directions.

2. REGULATION OF CHARGE DYNAMIC BEHAVIORS

AMCs EIL: In perovskite optoelectronic devices, the role of alkali metal compounds extends far beyond serving as A-site components of the perovskite lattice or bulk dopants for optimizing intrinsic optoelectronic properties.[16−21] In fact,

Received: October 30, 2025
Revised: January 28, 2026
Accepted: January 28, 2026
Published: February 6, 2026



ACS Publications © 2026 American Chemical Society

https://doi.org/10.1021/acsaelm.5c02309
ACS Appl. Electron. Mater. 2026, 8, 1456−1465

Downloaded from pubs.acs.org/aaembp/article-pdf/8/4/1456/6315647/el5c02309.pdf by SOUTHWEST JIAOTONG UNIV user on 07 November 2026

building on successful experiences in organic electronics, alkali metal compounds (e.g., LiF,[22−24] CsF,[25,26] Cs_2CO_3[27]) have long been widely employed as efficient electron injection layers deposited between the electron transport layer and metal electrodes (particularly low-work-function metals such as Al and Ag).[22−27] Their primary purpose is to significantly reduce electron injection barriers, optimize charge balance, and thereby enhance device current efficiency and reduce the operating voltage. However, despite repeated experimental validation and widespread application, the fundamental physicochemical mechanisms underlying this enhanced electron injection remain debated, with no consensus yet established. This mechanistic ambiguity has somewhat constrained our ability to rationally design and optimize such interfacial layers. Here, we systematically summarize and discuss this critical issue.

Quintero-Torres et al. discussed the enhancement mechanisms of LiF EIL in PeLEDs,[28] summarizing the widely recognized mechanisms as illustrated in Figure 1. (i) Dipole

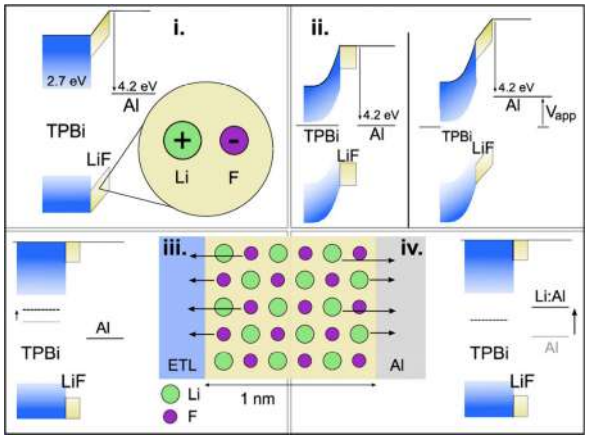


Figure 1. Possible mechanisms for enhanced cathode charge injection with LiF as EIL.[28] From i to iv are dipole moment effect, electron tunneling, N-type doping of the ETL, and low work function doping of cathode, respectively. Reproduced from ref 28. Copyright 2020, American Chemical Society.

Moment Effect: The significant electronegativity difference between F^- and Li^+ in LiF creates a strong intrinsic dipole moment, which induces misalignment between the cathode and the electron transport layer (ETL). An electrostatic potential drop beyond a fixed dipole moment has been observed across diverse material systems.[29−31] (ii) Electron tunneling: With a large band gap width (≈14.0 eV[32]), LiF can act as a high-resistance buffer layer. As a result, it exhibits a larger voltage drop than the adjacent layers (cathode and ETL), which can improve the energy level alignment between the cathode and ETL, and enable electron tunneling. (iii) N-type doping of the ETL: F^- ions from LiF may dissociate and migrate into the adjacent ETL, increasing the electron concentration within ETL.[33] (iv) Low work function doping of the cathode: Li^+ ions can dissociate and migrate into the cathode, thereby reducing the effective work function of the cathode.[34] Ultimately, they proposed that the enhanced injection in LiF-based systems stems from the migration and doping of F^- ions into the ETL and Li^+ ions into the Al cathode, collectively reducing both the width and height of the energy barrier and increasing the probability of electron tunneling.[28]

Additionally, numerous studies have described the mechanisms of the LiF EIL. For instance, LiF and other alkali metal halides in general are highly susceptible to radiation damage. Irradiation with quanta exceeding the band gap energy leads to efficient defect formation.[35] Therefore, Meskers et al. proposed that applying a moderate bias voltage with a potential difference smaller than the band gap causes the accumulation of trapped positive charges in the LiF layer, which further induces the efficient transport of electrons.[36] This is a defect-assisted charge transport mechanism, and this theory may help explain the unusual changes in carrier behavior within LEDs when an AMC interfacial layer is introduced outside the electron injection layer.[37]

While these findings are derived from studies on LiF, they can reasonably explain the enhancement mechanisms observed with other EIL materials such as CsF, Cs_2CO_3, and 8-hydroxyquinolinolatolithium (Liq). We emphasize that different AMCs EIL materials may align with specific theoretical models or result from the combined effects of multiple mechanisms. For example, unlike wide-bandgap, ionic EILs such as LiF, CsF, and Cs_2CO_3, metal−organic complex Liq EIL exhibits a bandgap of ≈3.0 eV and a LUMO level of ≈2.5 eV, making the charge tunneling concept insufficient to explain its charge injection improvement. Furthermore, although GeO_2 has a large bandgap like LiF, CsF, and Cs_2CO_3 EILs, but contains no alkali metal elements, the aforementioned framework (enhanced charge injection via tunneling effects) cannot account for the detrimental effects observed when using GeO_2 as EIL.[12] Furthermore, our analysis indicates that balanced injection cannot be achieved solely by tuning the thickness of a single EIL layer,[39] underscoring the complexity of the underlying multimechanistic interactions. However, quantifying the relative contribution of each potential mechanism remains challenging and falls beyond the scope of this review.

In addition, using AMCs as dopants can regulate charge injection by altering the work function of the transport layers. You et al. explored in depth the effect of CsCl doping on poly(3,4-ethylenedioxythiophene):poly(styrenesulfonate) (PEDOT:PSS).[38] As shown in Figure 2a and b, after CsCl doping, the PEDOT:PSS film transformed from a smooth, uniform amorphous state to a uniform and tightly packed crystalline state, which can promote charge transfer between conjugated polymers,[40,41] as illustrated in Figure 2c. XPS spectra (Figure 2d) indicated that the change in the chemical environment of S atoms in PEDOT:PSS is related to the phase segregation of PEDOT and PSS chains,[40] and the insulating PSS chains (the dominant species in the upper part of the film) are dragged away by the doped species, while PEDOT remains as the main conductive chain and adjusts its interactions and morphology. In Raman spectra (Figure 2e), the change in C_α=C_β stretching vibration on the PEDOT five-membered ring indicates that the resonance structure of PEDOT chains transforms from a benzoid structure to a quinoid-like structure, which may lead to the self-assembly of PEDOT into aggregates.[42] This results in enhanced conductivity and a change in work function due to the stacking and interaction of PEDOT chains,[43] as shown in Figure 2f. Therefore, the incorporation of the alkali metal salt CsCl can improve the efficiency of charge injection and transport in quasi-2D blue PeLEDs. Combined with the regulation of the perovskite film formation process by CsCl, the operational time T_{50} (the time required for the radiance to decrease to 50% of its initial value, 100 cd m^{-2}) of the targeted

Downloaded from pubs.acs.org/aaembp/article-pdf/8/4/1456/6315624/el5c02309.pdf by SOUTHWEST JIAOTONG UNIV user on 07 November 2026

https://doi.org/10.1021/acsaelm.5c02309
ACS Appl. Electron. Mater. 2026, 8, 1456−1465

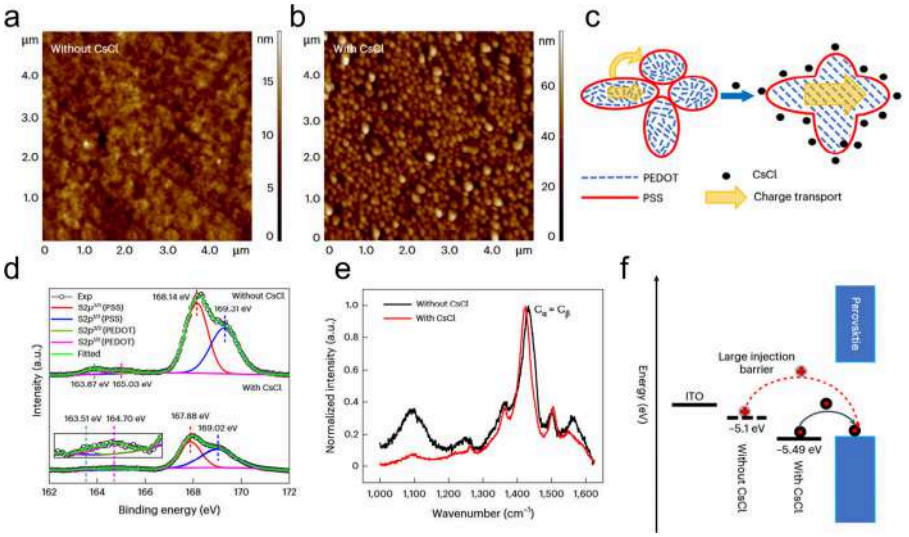


Figure 2. Effect of CsCl on properties of PEDOT:PSS films.[38] AFM images of PEDOT:PSS (a) without and (b) with CsCl. (c) Schematic diagram of the structural evolution of PEDOT:PSS after doping CsCl. (d) XPS spectra of pristine and CsCl-modified PEDOT:PSS films on ITO substrates. (e) Raman spectra of PEDOT:PSS films with and without CsCl. (f) Band alignment when using PEDOT:PSS with and without CsCl as the HIL for PeLEDs.[38] Reproduced with permission from ref 38. Copyright 2023 Springer Nature.

devices without encapsulation was estimated to be 5 min under continuous constant current density.[38] The improvement in stability can be attributed to fewer defects and optimized phase distribution induced by CsCl as well as better hole injection of CsCl-modified PEDOT:PSS.[38]

Furthermore, Huang et al. stated that after doping PEDOT:PSS with NaCl, its surface work function decreases, which is beneficial for hole injection and charge balance.[44] Wang et al. demonstrated the changes in interfacial energy band structure of PEDOT:PSS modified by different water-compatible alkali cations (Li, Na, K, Rb, Cs), with HOMO values of −5.42, −5.28, −5.34, −5.20, and −5.14 eV, respectively (the HOMO of undoped PEDOT:PSS is −5.01 eV).[45] Obviously, the energy level changes of PEDOT:PSS after doping with different AMCs stem from the phase separation and structural transformation of PEDOT:PSS itself. Notably, this enhanced hole injection through doping-induced changes in material structure and energy levels differs from the previously mentioned mechanism of AMCs thin films, facilitating electron injection. Furthermore, although a deeper HOMO level implies a higher hole injection efficiency, this does not mean that device performance will necessarily improve after doping. This is not only because both the doped PEDOT:PSS (as the concentration of doped NaCl gradually increased from 0 to 5 mg/mL, 10 and 15 mg/mL, the root-mean-square of the PEDOT:PSS surface gradually increased from 1.9 to 30 nm, 47 and 50 nm)[48] and perovskite films (after Na^+, K^+, and Cs^+ cations were doped into PEDOT:PSS, the RMS of the upper perovskite film increased from the initial 0.99 to 1.31 nm, 1.63 and 6.11 nm, respectively)[49] exhibit increased roughness to varying degrees, but also because additional ion migration pathways and more complex interactions are introduced.[46]

Inserting AMCs as functional layers can also regulate the charge dynamic behaviors. For example, Zeng et al. inserted a LiCl inorganic interfacial dipole layer between PEDOT:PSS and the $CsCu_2I_3$ EML, which can modulate the interfacial energy band structure, widen the hole injection barrier, and achieve delayed hole injection.[47] Yang et al. stated that introducing a 2 nm insulating LiF layer between the quasi-2D perovskite EML and the TPBi ETL is expected to block excess electrons, thereby improving charge balance.[48] In contrast, Chen et al. introduced a 1 nm LiF layer between $FAPbBr_3$ nanocrystals and the 4,6-bis(3,5-di-3-pyridinylphenyl)-2-methylpyrimidine (B3PymPm) ETL. We indicated that the Coulomb interaction between the defect-positive charge centers in the LiF layer and electrons enhanced electron injection,[37] which is similar to the defect-assisted charge transport mechanism mentioned before.[36] It can be found that even with the same AMC functional layer the resulting effects are completely opposite. We speculate that this difference arises from the varying properties of perovskites and transport layers, specifically due to the different chemical environments in which the AMC film is situated. Nevertheless, we believe that ion doping in AMCs under an electric field cannot be ignored in any system.

3. OPTIMIZATION OF CRYSTALLIZATION PROCESS

The performance of PeLEDs is fundamentally dependent on the morphology and quality of active layers. An ideal perovskite film should possess high coverage, uniform grain size, low defect density, and excellent crystalline orientation, which directly determine the nonradiative recombination losses and charge transport efficiency.[49−52] However, the crystallization process of perovskite films is complex and difficult to control, especially the nucleation and growth on nonideal substrates can easily generate pinholes and uneven grains, which become a bottleneck for performance improvement.

Among numerous strategies for regulating crystallization, the introduction of AMCs has demonstrated unique and powerful effects.Their action pathways can be mainly summarized into two core routes: First, serving as a direct interfacial modification layer, it is predeposited on the substrate to provide a physical or chemical template for perovskite crystallization. Second, acting as a functional additive, it is doped into the charge transport layer (e.g., PEDOT:PSS), and indirectly affects the nucleation and growth kinetics of

https://doi.org/10.1021/acsaelm.5c02309
ACS Appl. Electron. Mater. 2026, 8, 1456−1465

Downloaded from pubs.acs.org/aaembp/article-pdf/8/4/1456/6315624/el5c02309.pdf by SOUTHWEST JIAOTONG UNIV user on 07 November 2026

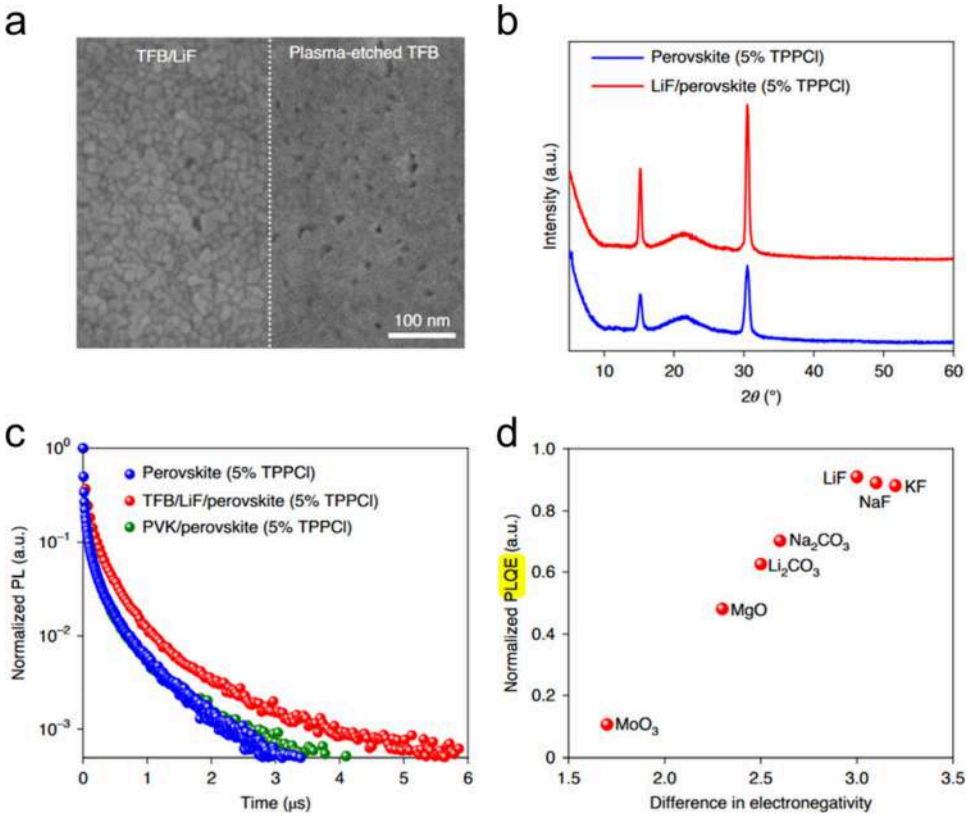


Figure 3. Effects of the LiF interfacial modifier.[53] (a) SEM images of perovskite films deposited on TFB/LiF and plasma-treated TFB surfaces. (b) XRD patterns and (c) time-resolved photoluminescence spectra of perovskite films deposited on different substrates. (d) Normalized PLQEs of perovskite films formed on a range of thermally evaporated interfacial materials with different polarities.[53] Reproduced with permission from ref 53. Copyright 2020 Springer Nature.

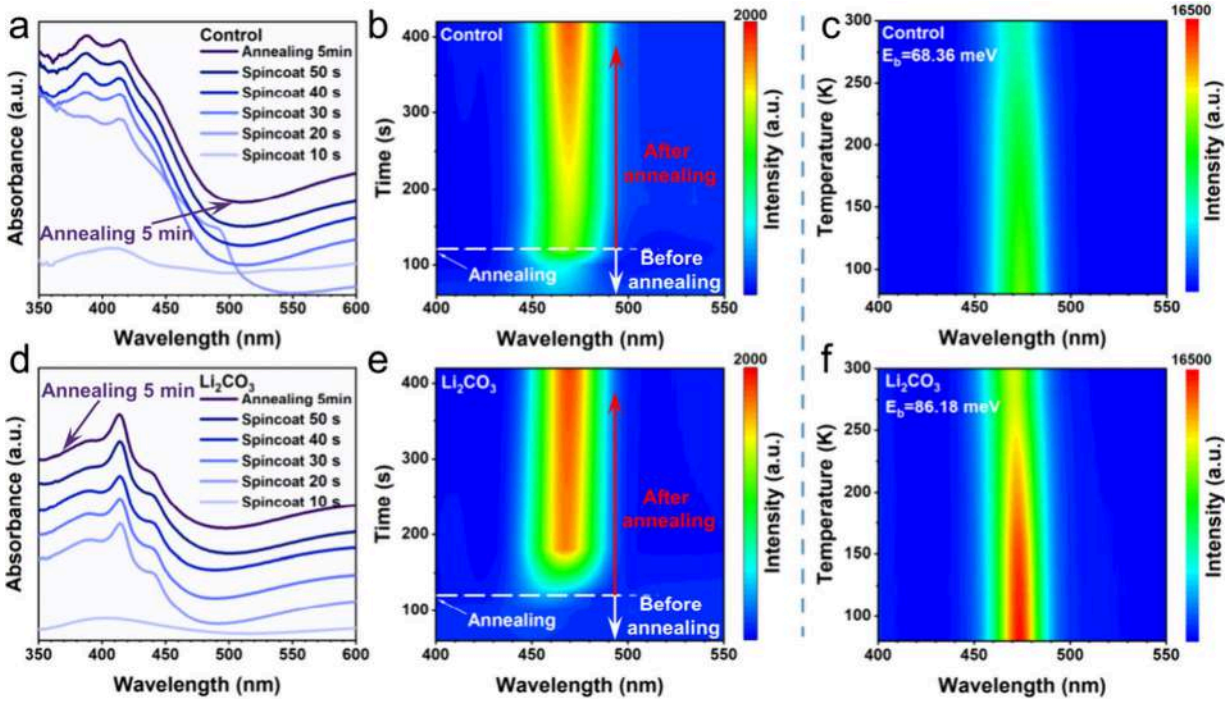


Figure 4. In situ evaluation of perovskite film growth process.[55] (a, d) UV−vis spectra of different spin-coatings and annealing times. (b, e) Time-dependent PL spectra. (c, f) Temperature-dependent PL spectra.[55] Reproduced or adapted from ref 55. Copyright 2024 American Chemical Society.

Downloaded from pubs.acs.org/aaembp/article-pdf/8/4/1456/6315647/ei5c02309.pdf by SOUTHWEST JIAOTONG UNIV user on 07 November 2026

https://doi.org/10.1021/acsaelm.5c02309
ACS Appl. Electron. Mater. 2026, 8, 1456−1465

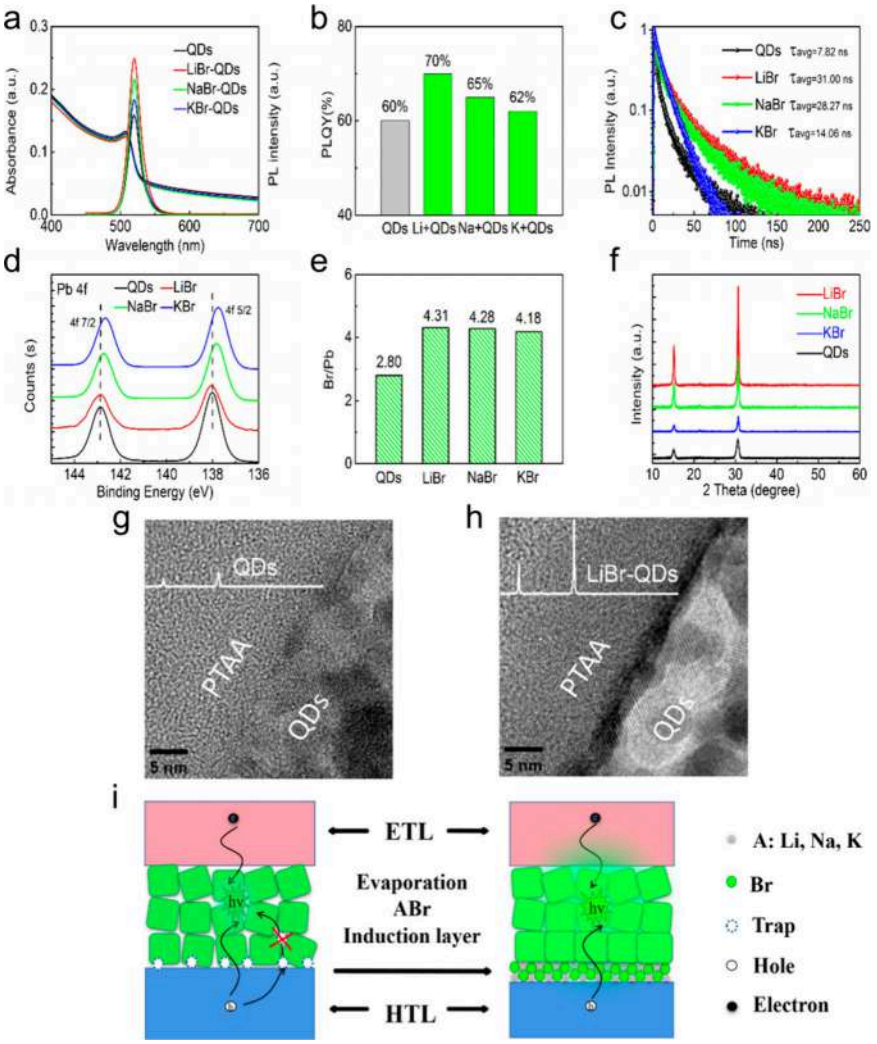


Figure 5. (a) Absorption and PL, (b) PLQY, (c) TRPL, (d) XPS, and (f) XRD spectra of PQDs spin-coated on different AMCs substrates, respectively.[57] (e) Atomic ratios of Br/Pb measured by XPS. (g, h) High-resolution TEM images at the interface of HTL/PQDs without and with a LiBr layer, respectively. Insets show the XRD spectra of original PQDs and LiBr-PQDs films. (i) Model of the AMCs interfacial modification layers strategy.[57] Reproduced with from ref 57. Copyright 2023 American Chemical Society.

perovskites on it by altering the surface properties of the substrates. Although these two strategies act at different sites, they ultimately converge to the same goal, guiding perovskites to form high-quality crystalline films. Herein, we sort out and compare the principles, phenomena, and effects of these two mechanisms.

AMCs Interfacial Modification Layers

Zhao et al.[53] discovered that inserting an ultrathin (≈1 nm) LiF interlayer enables the formation of perovskite films with excellent luminescent properties on incompatible hydrophobic charge transport materials (e.g., TFB). As shown in Figure 3a, perovskite films formed on the TFB/LiF interface exhibited larger and more distinct grains with a reduced pinhole density. Concurrently, the LiF layer enhanced the perovskite crystallinity (Figure 3b) and optical performance (Figure 3c). The variation in the photoluminescence quantum efficiency (PLQE) of perovskite films on different interfaces (Figure 3d) suggests that highly polar interfaces may provide effective templates for forming perovskite films with superior luminescence properties. Notably, while such correlations are observed, the possibility of chemical reactions between the perovskite layer and these materials cannot be ruled out. Similarly, introducing a LiF layer between PVK and the perovskite EML has proven beneficial for fabricating high-performance mini/micro-PeLEDs.[54] Researchers hypothesize that this improvement relates to fluorine forming hydrogen bonds with perovskite at the HTL/perovskite interface.[54]

Beyond facilitating the wettability of perovskite solutions, there are additional pathways through which AMCs' interfacial layers regulate the crystallization process. Zou et al.[55] found that the perovskite films already exhibited high photoluminescence (PL) intensity before annealing, and the PL stabilized after annealing, which indicate that the perovskite had crystallized prior to annealing (Figure 4b). However, after introduction of a Li_2CO_3 layer via spin-coating between PEDOT:PSS and the perovskite, the diffusion of Li^+ inhibited the binding between $[Pb(Br/Cl)_6]^{4-}$ and PEA during nucleation; in contrast, CO_3^{2-} replaced $[Pb(Br/Cl)_6]^{4-}$ octahedra to bind with PEA. These interactions were disrupted during annealing, and the unbound PEA continued to anchor in the perovskite film, manipulating the *n*-phase distribution (here *n* represents the number of lead-centered octahedra along the thickness direction in a single quantum well).

https://doi.org/10.1021/acsaelm.5c02309
ACS Appl. Electron. Mater. 2026, 8, 1456−1465

Downloaded from pubs.acs.org/aaembp/article-pdf/8/4/1456/6315624/el5c02309.pdf by SOUTHWEST JIAOTONG UNIV user on 07 November 2026

Consequently, after annealing the perovskite film, PL emerged and gradually increased (Figure 4e). Meanwhile, since the *n*-phase distribution is regulated during the nucleation stage rather than the crystal growth stage[56] (Figure 4a, b), the Li_2CO_3 layer can effectively regulate crystallization kinetics, suppress polydispersity in quantum well thickness, promote more uniform phase composition, thereby reducing non-radiative recombination losses in the perovskite film (Figure 4c, f). Therefore, the T_{50} of devices incorporating a Li_2CO_3 layer is extended by 2.56-fold compared to that of the control devices.

In contrast, for perovskite quantum dots (PQDs) EML, the nucleation of PQDs does not occur on the substrate, leading to fundamentally distinct mechanisms of the AMCs interlayer action. Li et al.[57] introduced functional layers of LiF and ABr (where A represents Li, Na, and K) between the HTL and PQDs via evaporation and found that the LiF layer did not improve the optical properties of the PQDs film, while the ABr film led to an increase in the Br/Pb ratio in the PQDs (Figure 5e). This indicates that the additional Br from ABr compensates for Br vacancies in the PQDs film. Consequently, the PL, PLQY, and TRPL spectra of the PQDs film improved to varying degrees after introduction of the ABr layers (Figure 5a–c). Moreover, due to the different sizes of the alkali metals, the extent of optical performance enhancement varied. Specifically, LiBr has the smallest molecular particle size and the highest density of Br per unit area, enabling more effective passivation of vacancy defects and resulting in the greatest improvement. Notably, as shown in Figure 5f, the diffraction peak positions of PQDs films with and without the ABr layer remained unchanged, indicating that the presence of ABr does not affect the crystal structure of the PQDs; that is, Li, Na, and K are not incorporated into the PQDs lattice. The authors supposed that the adsorption of alkali metal ions at the A-site on the PQD surface, combined with the filling of Br vacancies, leads to a chemical shift of Pb in the PQDs (Figure 5d). The enhancement in diffraction peak intensity arises from the exchange of long-chain ligands on the PQDs with short ABr molecules, which significantly reduces the distance between PQDs and promotes further crystal growth. High-resolution transmission electron microscopy (TEM) tests also showed that the inserted LiBr layer enhances the crystallinity of adjacent PQDs (Figure 5g, h). The discrete PQDs can be driven by the ABr substrate to grow into more compact, less defective, and higher-crystallinity PQD film (Figure 5i), which ultimately leads to a 2-fold improvement in the operational lifetime of devices incorporating a LiBr layer.[57]

In summary, we emphasize that alkali metal compound interfacial modification layers exhibit multifaceted and multi-level mechanisms in regulating perovskite film crystallization and quality that extend beyond merely improving wettability. Their specific functions are strongly dependent on the properties of the perovskite active layer (composition and morphology) and the chemical microenvironment at the interface.

AMCs Interfacial Dopants

Incorporating AMCs into charge transport layers, particularly in PEDOT:PSS solutions, not only enhances hole injection by adjusting the transport layer material structure and energy level as mentioned before, but also enables alkali metal cations to function as interfacial nucleation sites.[58] These sites actively induce perovskite nucleation and crystal growth, ultimately leading to the formation of high-quality films. As illustrated in Figure 6a, after doping PEDOT:PSS with K_2SO_4, K^+ ions

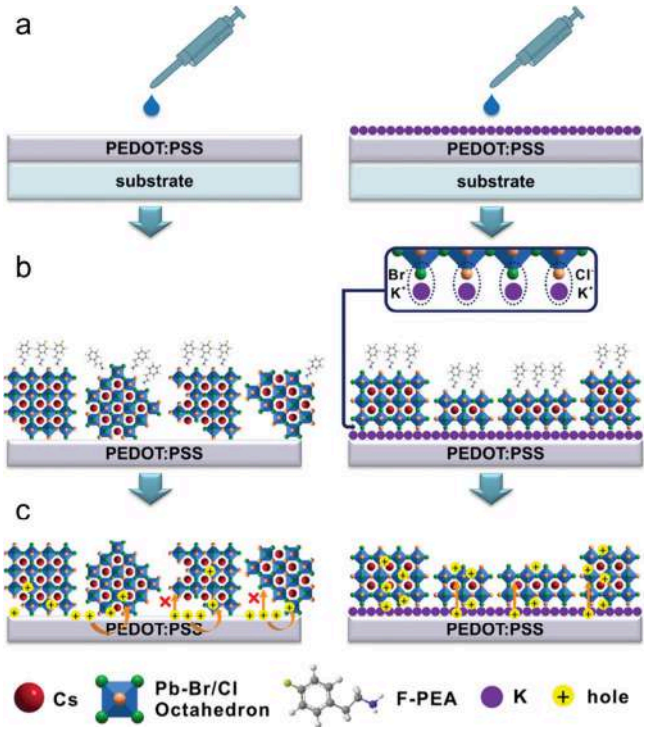


Figure 6. Schematic illustration of the K^+-guided grain growth and hole transport of perovskite films.[58] (a) Spin-coating of control and K^+-modified PEDOT:PSS films. (b) Crystal growth of perovskite grains on different substrates. (c) Hole transport characteristics from PEDOT:PSS to the perovskite. Reproduced with permission from ref 58. Copyright 2020 Wiley-VCH.

preferentially form K–Cl/Br bonds with halide ions on the PEDOT:PSS surface. This process not only passivates interfacial halide defects but also bridges PbX_2 octahedra (X = Br/Cl) with the underlying PEDOT:PSS substrate.[58] The PbX_2 octahedra anchor uniformly onto distributed K sites, further acting as nucleation seeds to guide the perovskite grain growth (Figure 6b). This interaction ultimately yields well-aligned perovskite assemblies with small-sized grains and controlled crystal orientation, alongside optimized charge transport pathways (Figure 6c), which leads to ≈4-fold improvement of T_{50} of K-modified devices.[58] Therefore, doping AMCs such as L-aspartic acid potassium (PLAK),[59] K_2SO_4,[60] and potassium sulfamate[61] into PEDOT:PSS of different systems can increase nucleation sites at the interface and improve the morphology and crystallinity of perovskite films.

Cs-based salts (e.g., CsBr,[62] Cs-TFSI,[63] CsCl[38]) similarly enhance perovskite film quality. You et al.[38] demonstrated that precipitated CsCl particles induce the formation of large-n phases in perovskite, triggering rearrangement of low-*n* phases in quasi-2D perovskites. Notably, adding CsCl directly to the perovskite precursor failed to achieve phase redistribution, indicating that the chemically active CsCl particles precipitated on PEDOT:PSS are responsible for directing the perovskite growth and phase modulation. In contrast, rubidium chloride (RbCl) under identical conditions could not induce phase modulation in quasi-2D perovskite, attributable to its inertness toward precursor.[38]

https://doi.org/10.1021/acsaelm.5c02309
ACS Appl. Electron. Mater. 2026, 8, 1456–1465

Downloaded from pubs.acs.org/aaembp/article-pdf/8/4/1456/6315624/el5c02309.pdf by SOUTHWEST JIAOTONG UNIV user on 07 November 2026

Recently, Cao et al.[64] incorporated lithium salicylate (SAL) as a reactive initiator into the perovskite precursor. A proton exchange reaction between PEDOT:PSS and SAL formed a multifunctional PSS-Li interlayer, regulating the perovskite nucleation and growth. However, systematic studies on the impact of other AMCs doped into PEDOT:PSS on perovskite crystallization remain scarce. Interestingly, we found that although the types of AMCs dopants are different, they are all believed to inhibit the formation of the small *n*-phase,[38,60,61] the underlying mechanism remains unclear unfortunately. We also note that K-based AMCs dopants appear more prevalent for modulating perovskite nucleation, potentially due to the intrinsic properties of alkali metal ions (e.g., ionic radius, chemical reactivity, and migration capability).

4. OTHER ROLES OF AMCS INTERFACES

The passivation effects of AMCs on perovskite interfaces primarily stem from their functional anions,[38,61,63−65] operating through mechanisms such as halide vacancy filling or coordination with undercoordinated Pb^{2+}. In contrast, the influence of alkali metal cations on defects is more reflected in the modulation of *n*-phase distribution, as phase engineering plays a critical role in controlling trap states.[66−69] Additionally, LiF interlayer can prevent direct contact between perovskite and ETL, thereby suppressing interfacial quenching.[48,70] Ultrathin LiF layer inserted on PEDOT:PSS reduce film pinholes and inhibit exciton quenching.[71] Thus, the defect passivation by AMCs is a multipath synergistic process. Despite numerous research achievements, significant ambiguity and gaps remain in the mechanistic study, which will be discussed later.

Furthermore, AMCs interlayers enable novel device architectures. For instance, Wu et al. designed an innovative "insulator-perovskite-insulator" (IPI) structure for PeLEDs.[72−74] In this structure, the traditional hole injection layer (PEDOT:PSS) or its combination with PVK (PEDOT:PSS/PVK) is replaced with an ultrathin insulating LiF film, which is sandwiched on the perovskite film. This configuration not only blocks leakage current and confines charge recombination within the perovskite but also suppresses exciton quenching at the perovskite/charge transport layer interfaces, enhancing radiative recombination efficiency.[72−74] In addition, using a LiF/Al/Ag/LiF semitransparent electrode (where LiF/Al reduces the work function, and the LiF above the Ag acts as a blocking layer to suppress PL quenching at the interface), a high-performance white PeLED with significantly enhanced light extraction efficiency can be constructed.[75]

5. SUMMARY AND OUTLOOK

This review has systematically discussed the multidimensional interfacial regulation effects of AMCs in PeLEDs. Many investigations indicate that AMCs have evolved from their early role as a single electron injection layer to an integrated multifunctional interface engineering material that combines the regulation of charge dynamic behavior, crystallization control, defect passivation, and even light field manipulation. Their key roles can be summarized as the following two core aspects: (i) Acting as a "regulator" of charge behaviors: Through pathways such as the dipole moment effect, electron tunneling effect, n-type doping of the ETL, and low-work-function metal doping of the cathode, AMCs can function as independent charge injection layers/functional interfacial layers to optimize the balance of charge injection. Meanwhile, doping transport layers with AMCs can adjust interfacial energy levels to achieve improved injection and transport. (ii) Acting as a "guide" of the crystallization process: Whether used as a direct interfacial layer or a transport layer dopant, AMCs can effectively guide the formation of high-quality perovskite films with more complete coverage and better phase distribution by altering the substrate surface energy, participating in the formation of intermediate phases, or regulating nucleation kinetics. In addition, we analyzed the mechanisms of AMCs for perovskite defect passivation and discussed novel device structures constructed by using AMCs (especially LiF).

Despite the remarkable progress achieved in related research, a review of the current development of this field reveals that several key scientific issues and technical challenges still require in-depth exploration. First, numerous gaps remain in our understanding of the mechanisms of AMCs. For instance, when devices operate long-term under electric field, light irradiation, and thermal stress conditions, the ion migration behavior, pathways, and consequent effects of AMCs in the interfacial layer remain unclear, yet this is of great significance for PeLEDs. Therefore, future research may need to leverage in situ and real-time characterization techniques and first-principles calculations to directly capture the evolution of interfacial structures, ion migration pathways, and real-time processes of passivation reactions during dynamic processes. Second, current research is excessively focused on a limited number of materials (e.g., K^+ salts and LiF). In the future, the library of AMCs should be systematically expanded, covering combinations of different cations with a wider range of anions. Furthermore, greater attention should be paid to the intrinsic properties of the AMCs materials. For example, insufficient surface coverage often leads to increased leakage current, further resulting in the formation of short-circuit paths and device failure.[76] For subnanometer-scale AMCs films (typically 1−2 nm thick), they often exhibit an incompletely covered island-like structure.[77,78] Additionally, AMCs like LiF generate optically and electrically active defects, color centers, and hardening sites under radiation or heating.[78−81] Although these intrinsic properties are crucial for precisely controlling charge dynamics by AMCs, they are often easily overlooked.

AUTHOR INFORMATION

Corresponding Authors

Wen Li − *Key Laboratory of Advanced Technologies of Materials (Ministry of Education), School of Materials Science and Engineering, Southwest Jiaotong University, Chengdu 610031, P. R. China;* orcid.org/0000-0002-2805-3230; Email: liwen3337@swjtu.edu.cn

Weiqing Yang − *Key Laboratory of Advanced Technologies of Materials (Ministry of Education), School of Materials Science and Engineering, Southwest Jiaotong University, Chengdu 610031, P. R. China; Research Institute of Frontier Science, Southwest Jiaotong University, Chengdu 610031, P. R. China;* orcid.org/0000-0001-8828-9862; Email: wqyang@swjtu.edu.cn

Authors

Yongjian Chen − *Key Laboratory of Advanced Technologies of Materials (Ministry of Education), School of Materials Science and Engineering, Southwest Jiaotong University, Chengdu 610031, P. R. China*

Downloaded from pubs.acs.org/aaembp/article-pdf/8/4/1456/6315624/el5c02309.pdf by SOUTHWEST JIAOTONG UNIV user on 07 November 2026

https://doi.org/10.1021/acsaelm.5c02309
ACS Appl. Electron. Mater. 2026, 8, 1456−1465

Xiankan Zeng − *Key Laboratory of Advanced Technologies of Materials (Ministry of Education), School of Materials Science and Engineering, Southwest Jiaotong University, Chengdu 610031, P. R. China*

Complete contact information is available at: https://pubs.acs.org/10.1021/acsaelm.5c02309

Notes

The authors declare no competing financial interest.

■ ACKNOWLEDGMENTS

This work was in part supported by the National Natural Science Foundation of China (No. 52202188) and National Key Research and Development Program Young Scientist Project (2023YFB3405700).

■ REFERENCES

(1) Tan, Z.-K.; Moghaddam, R. S.; Lai, M. L.; Docampo, P.; Higler, R.; Deschler, F.; Price, M.; Sadhanala, A.; Pazos, L. M.; Credgington, D.; Hanusch, F.; Bein, T.; Snaith, H. J.; Friend, R. H. Bright Light-Emitting Diodes Based on Organometal Halide Perovskite. *Nat. Nanotechnol.* **2014**, *9* (9), 687−692.

(2) Kong, L.; Luo, Y.; Wu, Q.; Xiao, X.; Wang, Y.; Chen, G.; Zhang, J.; Wang, K.; Choy, W. C. H.; Zhao, Y.-B.; Li, H.; Chiba, T.; Kido, J.; Yang, X. Efficient and Stable Hybrid Perovskite-Organic Light-Emitting Diodes with External Quantum Efficiency Exceeding 40 per Cent. *Light Sci. Appl.* **2024**, *13* (1), 138.

(3) So, F.; Kondakov, D. Degradation Mechanisms in Small-Molecule and Polymer Organic Light-Emitting Diodes. *Adv. Mater.* **2010**, *22* (34), 3762−3777.

(4) Coburn, C.; Forrest, S. R. Effects of Charge Balance and Exciton Confinement on the Operational Lifetime of Blue Phosphorescent Organic Light-Emitting Diodes. *Phys. Rev. Applied* **2017**, *7* (4), 041002.

(5) Chen, S.; Jiang, X.; So, F. Hole Injection Polymer Effect on Degradation of Organic Light-Emitting Diodes. *Org. Electron.* **2013**, *14* (10), 2518−2522.

(6) Zhang, L.; Yang, X.; Jiang, Q.; Wang, P.; Yin, Z.; Zhang, X.; Tan, H.; Yang, Y.; Wei, M.; Sutherland, B. R.; Sargent, E. H.; You, J. Ultra-Bright and Highly Efficient Inorganic Based Perovskite Light-Emitting Diodes. *Nat. Commun.* **2017**, *8* (1), 15640.

(7) Jeong, J.-E.; Park, J. H.; Jang, C. H.; Song, M. H.; Woo, H. Y. Multifunctional Charge Transporting Materials for Perovskite Light-Emitting Diodes. *Adv. Mater.* **2020**, *32* (51), 2002176.

(8) Islam, A.; Shah, S. H. U.; Haider, Z.; Imran, M.; Li, M.-D. Organic Hole-Transport Layers: An Innovative Approach for Efficient Perovskite Light-Emitting Diodes. *Advanced Optical Materials* **2024**, *12* (17), 2303304.

(9) Guo, K.; Ren, L.; Chen, C.; Tang, Z.; Niu, X.; Kong, L.; Xue, T.; Ding, L.; Wang, S.; Zhang, F.; Yang, X. High-Brightness Blue Perovskite Light-Emitting Diodes With Low Efficiency Roll-Off Enabled by Dual-ETL and Hole Transport Regulation. *Advanced Optical Materials* **2025**, *13* (14), 2403483.

(10) Han, T.-H.; Tan, S.; Xue, J.; Meng, L.; Lee, J.-W.; Yang, Y. Interface and Defect Engineering for Metal Halide Perovskite Optoelectronic Devices. *Adv. Mater.* **2019**, *31* (47), 1803515.

(11) Chen, Z.; Li, Z.; Hopper, T. R.; Bakulin, A. A.; Yip, H.-L. Materials, Photophysics and Device Engineering of Perovskite Light-Emitting Diodes. *Rep. Prog. Phys.* **2021**, *84* (4), 046401.

(12) Schmitz, C.; Schmidt, H.-W.; Thelakkat, M. Lithium-Quinolate Complexes as Emitter and Interface Materials in Organic Light-Emitting Diodes. *Chem. Mater.* **2000**, *12* (10), 3012−3019.

(13) Hung, L. S.; Tang, C. W.; Mason, M. G. Enhanced Electron Injection in Organic Electroluminescence Devices Using an Al/LiF Electrode. *Appl. Phys. Lett.* **1997**, *70* (2), 152−154.

(14) Kausar, A.; Sattar, A.; Xu, C.; Zhang, S.; Kang, Z.; Zhang, Y. Advent of Alkali Metal Doping: A Roadmap for the Evolution of Perovskite Solar Cells. *Chem. Soc. Rev.* **2021**, *50* (4), 2696−2736.

(15) Li, Y.; Lou, Y.-H.; Zhou, Y.-H.; Xia, Y.; Wang, B.; Wang, Z.-K. Review on the Promising Roles of Alkali Metals toward Highly Efficient Perovskite Light-Emitting Diodes. *J. Mater. Chem. C* **2023**, *11* (6), 2011−2025.

(16) Yang, Y.; Xu, S.; Ni, Z.; Van Brackle, C. H.; Zhao, L.; Xiao, X.; Dai, X.; Huang, J. Highly Efficient Pure-Blue Light-Emitting Diodes Based on Rubidium and Chlorine Alloyed Metal Halide Perovskite. *Adv. Mater.* **2021**, *33* (33), 2100783.

(17) Ko, P. K.; Chen, D.; Li, C.-H. A.; Chan, C. C. S.; Sergeev, A.; Ding, P.; Lam, D.; Ouyang, B.; Guo, L.; Wong, K. S.; Halpert, J. E. Color Tuning in Cesium Lead Halide Nanocrystals via A-Site Substitution as an Alternative Method for Achieving Spectrally Stable Blue Perovskite Nanocrystal Light-Emitting Diodes. *Chem. Mater.* **2024**, *36* (8), 3735−3744.

(18) Shi, C.; Zhang, H.; Li, H.; Fu, H. Achieving Tunable Amplified Spontaneous Emission in Rb-Cs Alloyed Quasi-2D Perovskites with Low Threshold and Exceptional Spectral Stability. *Adv. Mater.* **2025**, *37* (35), 2504029.

(19) Chen, Y.; Wang, R.; Kusch, G.; Xu, B.; Hao, C.; Xue, C.; Cheng, L.; Zhu, L.; Wang, J.; Li, H.; Oliver, R. A.; Wang, N.; Huang, W.; Wang, J. All-Site Alloyed Perovskite for Efficient and Bright Blue Light-Emitting Diodes. *Nat. Commun.* **2025**, *16* (1), 3254.

(20) Guan, Z.; Li, Y.; Zhu, Z.; Zeng, Z.; Chen, Z.; Ren, Z.; Li, G.; Tsang, S.; Yip, H.; Xiong, Y.; Lee, C. High-Efficiency Blue Perovskite Light-Emitting Diodes with Improved Photoluminescence Quantum Yield via Reducing Trap-Induced Recombination and Exciton-Exciton Annihilation. *Adv. Funct Materials* **2022**, *32* (40), 2203962.

(21) Guo, Z.; Zhang, Y.; Wang, B.; Wang, L.; Zhou, N.; Qiu, Z.; Li, N.; Chen, Y.; Zhu, C.; Xie, H.; Song, T.; Song, L.; Xue, H.; Tao, S.; Chen, Q.; Xing, G.; Xiao, L.; Liu, Z.; Zhou, H. Promoting Energy Transfer via Manipulation of Crystallization Kinetics of Quasi-2D Perovskites for Efficient Green Light-Emitting Diodes. *Adv. Mater.* **2021**, *33* (40), 2102246.

(22) Chen, J.; Liu, X.; Cai, B.; Cheng, Y.; Wen, H.; Zhu, D.; Xiong, Y.; Dai, L.; Yan, X.; Xiang, B.; Luo, X.; Feng, W.; Du, J.; Dong, S.; Shan, Q.; Chen, S.; Zeng, H.; Xiong, Q.; Duan, L.; Ma, D. Lattice-Matched Molecular-Anchor Design for High-Performance Perovskite Quantum Dot Light-Emitting Diodes. *Nat. Commun.* **2025**, *16* (1), 8201.

(23) Peng, C.; Yao, H.; Ali, O.; Chen, W.; Yang, Y.; Huang, Z.; Liu, H.; Li, J.; Chen, T.; Li, Z.; Sun, M.; Zhou, H.; Tao, X.; Wang, N.; Wang, J.; Xiao, Z. Weakly Space-Confined All-Inorganic Perovskites for Light-Emitting Diodes. *Nature* **2025**, *643* (8070), 96−103.

(24) Jiang, Y.; Sun, C.; Xu, J.; Li, S.; Cui, M.; Fu, X.; Liu, Y.; Liu, Y.; Wan, H.; Wei, K.; Zhou, T.; Zhang, W.; Yang, Y.; Yang, J.; Qin, C.; Gao, S.; Pan, J.; Liu, Y.; Hoogland, S.; Sargent, E. H.; Chen, J.; Yuan, M. Synthesis-on-Substrate of Quantum Dot Solids. *Nature* **2022**, *612* (7941), 679−684.

(25) Liu, Z.; Qiu, W.; Peng, X.; Sun, G.; Liu, X.; Liu, D.; Li, Z.; He, F.; Shen, C.; Gu, Q.; Ma, F.; Yip, H.; Hou, L.; Qi, Z.; Su, S. Perovskite Light-Emitting Diodes with EQE Exceeding 28% through a Synergetic Dual-Additive Strategy for Defect Passivation and Nanostructure Regulation. *Adv. Mater.* **2021**, *33* (43), 2103268.

(26) Liu, D.; Nie, X.; Li, X.-G.; Li, D.-L.; Chen, Z.; Liao, S.; Sun, G.; Liang, B.; Yang, Z.; Wang, Z.; Li, M.; Li, M.-D.; Kido, J.; Su, S.-J. Highly Efficient Perovskite/Organic Hybrid White Electroluminescent Devices with Extended Operational Lifetime and Wide Color Gamut. *Adv. Mater.* **2025**, *37* (38), 2507820.

(27) Chi, S.; Chen, Y.; Li, X.; Wang, J.; Zhao, Z.; Li, Z.; Miao, Y.; Tong, X.; Liu, J.; Bi, Y.; Liu, Z.; Wang, Z.; Yang, W.; Lin, K. Functional Molecule Surface Infiltration Treatment for Efficient All-Inorganic Perovskite Light-Emitting Diodes. *Chemical Engineering Journal* **2025**, *514*, 162787.

(28) Quintero-Bermudez, R.; Kirman, J.; Ma, D.; Sargent, E. H.; Quintero-Torres, R. Mechanisms of LiF Interlayer Enhancements of

Downloaded from pubs.acs.org/aaemb/article-pdf/8/4/1456/6316247/el5c02309.pdf by SOUTHWEST JIAOTONG UNIV user on 07 November 2026

Perovskite Light-Emitting Diodes. *J. Phys. Chem. Lett.* **2020**, *11* (10), 4213−4220.
(29) Vázquez, H.; Gao, W.; Flores, F.; Kahn, A. Energy Level Alignment at Organic Heterojunctions: Role of the Charge Neutrality Level. *Phys. Rev. B* **2005**, *71* (4), 041306.
(30) Campbell, I. H.; Rubin, S.; Zawodzinski, T. A.; Kress, J. D.; Martin, R. L.; Smith, D. L.; Barashkov, N. N.; Ferraris, J. P. Controlling Schottky Energy Barriers in Organic Electronic Devices Using Self-Assembled Monolayers. *Phys. Rev. B* **1996**, *54* (20), R14321−R14324.
(31) Quintero-Bermudez, R.; Proppe, A. H.; Mahata, A.; Todorović, P.; Kelley, S. O.; De Angelis, F.; Sargent, E. H. Ligand-Induced Surface Charge Density Modulation Generates Local Type-II Band Alignment in Reduced-Dimensional Perovskites. *J. Am. Chem. Soc.* **2019**, *141* (34), 13459−13467.
(32) Sirdeshmukh, D. B.; Sirdeshmukh, L.; Subhadra, K. G. *Alkali Halides: A Handbook of Physical Properties*; Hull, R., Osgood, R. M., Sakaki, H., Zunger, A., Series Eds.; Springer Series in Materials Science; Springer Berlin Heidelberg: Berlin, Heidelberg, 2001; Vol. *49*. DOI: 10.1007/978-3-662-04341-7.
(33) Heil, H.; Steiger, J.; Karg, S.; Gastel, M.; Ortner, H.; Von Seggern, H.; Stößel, M. Mechanisms of Injection Enhancement in Organic Light-Emitting Diodes through an Al/LiF Electrode. *J. Appl. Phys.* **2001**, *89* (1), 420−424.
(34) Shaheen, S. E.; Jabbour, G. E.; Morrell, M. M.; Kawabe, Y.; Kippelen, B.; Peyghambarian, N.; Nabor, M.-F.; Schlaf, R.; Mash, E. A.; Armstrong, N. R. Bright Blue Organic Light-Emitting Diode with Improved Color Purity Using a LiF/Al Cathode. *J. Appl. Phys.* **1998**, *84* (4), 2324−2327.
(35) Montereali, R. M. Point Defects in Thin Insulating Films of Lithium Fluoride for Optical Microsystems. In *Handbook of Thin Films*; Elsevier, 2002; pp 399−431. DOI: 10.1016/B978-012512908-4/50043-6.
(36) Bory, B. F.; Gomes, H. L.; Janssen, R. A. J.; De Leeuw, D. M.; Meskers, S. C. J. Electrical Conduction of LiF Interlayers in Organic Diodes. *J. Appl. Phys.* **2015**, *117* (15), 155502.
(37) Chen, Y.; Yan, C.; Chen, Z.; Zeng, X.; Wang, Q.; Yang, S.; Pan, L.; Li, C.; Mu, M.; Li, W.; Tang, G.; Yang, W. Interfacial Coulomb-Enhanced Charge Injection for Efficient Perovskite Light-Emitting Diodes. *Materials Today Physics* **2024**, *43*, 101413.
(38) Chu, Z.; Zhang, W.; Jiang, J.; Qu, Z.; Ma, F.; Zhao, Y.; Chu, X.; Shen, Y.; Li, Y.; Yin, Z.; Zhang, X.; You, J. Blue Light-Emitting Diodes Based on Quasi-Two-Dimensional Perovskite with Efficient Charge Injection and Optimized Phase Distribution via an Alkali Metal Salt. *Nat. Electron* **2023**, *6* (5), 360−369.
(39) Chen, Y.; Qu, Y.; Huang, L.; Zeng, X.; Zhang, H.; Li, W.; Tang, G.; Xiao, X.; Yang, W. Organic/Inorganic Heterointerfaces Engineering for Balanced Charge Distribution. *Materials Today Physics* **2025**, *56*, 101764.
(40) Liu, X.; Li, B.; Zhang, N.; Yu, Z.; Sun, K.; Tang, B.; Shi, D.; Yao, H.; Ouyang, J.; Gong, H. Multifunctional RbCl Dopants for Efficient Inverted Planar Perovskite Solar Cell with Ultra-High Fill Factor, Negligible Hysteresis and Improved Stability. *Nano Energy* **2018**, *53*, 567−578.
(41) Thomas, J. P.; Zhao, L.; McGillivray, D.; Leung, K. T. High-Efficiency Hybrid Solar Cells by Nanostructural Modification in PEDOT:PSS with Co-Solvent Addition. *J. Mater. Chem. A* **2014**, *2* (7), 2383−2389.
(42) Ouyang, J.; Xu, Q.; Chu, C.-W.; Yang, Y.; Li, G.; Shinar, J. On the Mechanism of Conductivity Enhancement in Poly(3,4-Ethylenedioxythiophene):Poly(Styrene Sulfonate) Film through Solvent Treatment. *Polymer* **2004**, *45* (25), 8443−8450.
(43) Lin, Y.-J.; Yang, F.-M.; Huang, C.-Y.; Chou, W.-Y.; Chang, J.; Lien, Y.-C. Increasing the Work Function of Poly(3,4-Ethylenedioxythiophene) Doped with Poly(4-Styrenesulfonate) by Ultraviolet Irradiation. *Appl. Phys. Lett.* **2007**, *91* (9), 092127.
(44) Huang, X.; Bäuerle, R.; Scherz, F.; Tisserant, J.-N.; Kowalsky, W.; Lovrinčić, R.; Hernandez-Sosa, G. Improved Performance of Perovskite Light-Emitting Diodes with a NaCl Doped PEDOT:PSS Hole Transport Layer. *J. Mater. Chem. C* **2021**, *9* (12), 4344−4350.
(45) Wang, H.; Hu, S.; Li, H.; Guo, Y.; Zhao, G.; Liu, P.; Gao, J.; Cheng, Z.; Tong, Y.; Qi, H.; Zhang, Y.; Wang, H. Alkali Cations Modified Poly(Styrene Sulfonate) Enabling Interfacial Band Structure Regulation for Efficient True-Blue Perovskite Light-Emitting Diodes. *Org. Electron.* **2023**, *114*, 106746.
(46) Zeng, X.; Yan, C.; Wang, Q.; Cao, J.; Fu, X.; Yang, S.; Chen, Y.; Pan, L.; Li, W.; Yang, W. High Curvature PEDOT:PSS Transport Layer Toward Enhanced Perovskite Light-Emitting Diodes. *Small* **2023**, *19* (47), 2304411.
(47) Zeng, X.; Yin, Q.; Pan, L.; Chen, Y.; Li, C.; Mu, M.; Wang, Q.; Li, W.; Yang, W. Hole Delayed-Release Effect of Inorganic Interfacial Dipole Layer on Charge Balance for Boosting CsCu2I3 Light-Emitting Diodes. *ACS Nano* **2025**, *19* (12), 11878−11890.
(48) You, M.; Wang, H.; Cao, F.; Zhang, C.; Zhang, T.; Kong, L.; Wang, L.; Zhao, D.; Zhang, J.; Yang, X. Improving Efficiency and Stability in Quasi-2D Perovskite Light-Emitting Diodes by a Multifunctional LiF Interlayer. *ACS Appl. Mater. Interfaces* **2020**, *12* (38), 43018−43023.
(49) Vila, M.; Bartolomé, J.; El Astal-Quirós, A.; Martínez-Pastor, J. P.; Suarez, I.; de Andrés, A.; Coya, C. Morphology Engineering of MAPbBr3 Thin Films for Enhanced Lighting Applications. *APL Materials* **2025**, *13* (7), 071109.
(50) Liu, W.; Qiao, Y.; Deng, Y.; Zhang, Y.; Liu, C.; Guo, W. Advancements and Challenges of Highly Efficient and Stable Perovskite Light-Emitting Diodes. *Laser & Photonics Reviews* **2026**, *20* (2), e01787.
(51) Sun, C.; Jiang, Y.; Cui, M.; Qiao, L.; Wei, J.; Huang, Y.; Zhang, L.; He, T.; Li, S.; Hsu, H.-Y.; Qin, C.; Long, R.; Yuan, M. High-Performance Large-Area Quasi-2D Perovskite Light-Emitting Diodes. *Nat. Commun.* **2021**, *12* (1), 2207.
(52) Shen, C.; Fang, S.; Zhang, J.; Liang, X.; Su, C.; Qing, J.; Cai, W.; Luo, Y.; Yang, R.; Hou, L. High Performance and Stable Pure-Blue Quasi-2D Perovskite Light-Emitting Diodes by Multifunctional Zwitterionic Passivation Engineering. *Adv. Photon.* **2024**, *6* (02), 026002.
(53) Zhao, B.; Lian, Y.; Cui, L.; Divitini, G.; Kusch, G.; Ruggeri, E.; Auras, F.; Li, W.; Yang, D.; Zhu, B.; Oliver, R. A.; MacManus-Driscoll, J. L.; Stranks, S. D.; Di, D.; Friend, R. H. Efficient Light-Emitting Diodes from Mixed-Dimensional Perovskites on a Fluoride Interface. *Nat. Electron* **2020**, *3* (11), 704−710.
(54) Hsu, C.; Tian, S.; Lian, Y.; Zhang, G.; Zhou, Q.; Cao, X.; Zhao, B.; Di, D. Efficient Mini/Micro-Perovskite Light-Emitting Diodes. *Cell Reports Physical Science* **2021**, *2* (9), 100582.
(55) Zhuang, D.; Wang, Y.; Cai, Q.; Zhai, L.; Huang, H.; Yang, G.; Yang, Y.; Zhang, L.; Zou, C. Restraint of Nonradiative Recombination via Modulation of N-Phase Distribution through Interfacial Lithium Salt Insertion for High-Performance Pure-Blue Perovskite LEDs. *ACS Appl. Mater. Interfaces* **2024**, *16* (24), 31274−31282.
(56) Guo, Z.; Liang, Y.; Ni, D.; Li, L.; Liu, S.; Zhang, Y.; Chen, Q.; Zhang, Q.; Wang, Q.; Zhou, H. Homogeneous Phase Distribution in Q-2D Perovskites via Co-Assembly of Spacer Cations for Efficient Light-Emitting Diodes. *Adv. Mater.* **2023**, *35* (38), 2302711.
(57) Yang, K.; Zheng, J.; Mao, J.; Zhao, H.; Ju, S.; Zhang, Q.; Lin, Z.; Yu, Y.; Li, F. Interface-Induced Crystallinity Enhancement of Perovskite Quantum Dots for Highly Efficient Light-Emitting Diodes. *ACS Appl. Mater. Interfaces* **2023**, *15* (33), 40062−40069.
(58) Shen, Y.; Shen, K.-C.; Li, Y.-Q.; Guo, M.; Wang, J.; Ye, Y.; Xie, F.-M.; Ren, H.; Gao, X.; Song, F.; Tang, J.-X. Interfacial Potassium-Guided Grain Growth for Efficient Deep-Blue Perovskite Light-Emitting Diodes. *Adv. Funct. Mater.* **2021**, *31* (6), 2006736.
(59) Yang, K.; Lin, Q.; Xu, B.; Yu, Y.; Hu, H.; Li, F. Synergistic Interaction of Multi-Functional Additives at the Buried Interface for Efficient Blue Perovskite Light-Emitting Diodes. *J. Mater. Chem. C* **2024**, *12* (11), 4123−4129.
(60) Tang, J.; Zhang, G.; Wang, C.; Deng, L.; Zhu, X.; Yu, H.; Wang, K.; Li, J. Investigation of the Role of K2SO4 Electrolyte in Hole

Downloaded from pubs.acs.org/aaembp/article-pdf/8/4/1456/6315247/ei5c02309.pdf by SOUTHWEST JIAOTONG UNIV user on 07 November 2026

Transport Layer for Efficient Quasi-2D Perovskite Light-Emitting Diodes. *J. Phys. Chem. Lett.* **2024**, *15* (4), 1112−1120.
(61) Yu, Y.; Wang, B.-F.; Shen, Y.; Su, Z.-H.; Zhang, K.; Ren, H.; Zhang, Y.-F.; Gao, X.; Tang, J.-X.; Li, Y.-Q. Regulating Perovskite Crystallization through Interfacial Engineering Using a Zwitterionic Additive Potassium Sulfamate for Efficient Pure-Blue Light-Emitting Diodes. *Angew. Chem., Int. Ed.* **2024**, *63* (7), No. e202319730.
(62) He, H.; Ai, Y.; Shen, P.; Wang, Z.; Zhang, H.; Zhou, Y.; Mei, F. Enhanced Performance of Perovskite Light-Emitting Diodes with PEDOT:PSS/CsBr Composite Hole Transport Layer. *Opt. Mater.* **2024**, *153*, 115638.
(63) Zhou, H.; Ma, Y.; Wang, Y.; Liu, L.; Cheng, G.; Chen, S. Cs-TFSI-Modified PEDOT:PSS Interface Engineering for High-Performance Sky-Blue Perovskite Light-Emitting Diodes: Achieving Optimal Energy Alignment and Defect Suppression. *ACS Appl. Electron. Mater.* **2025**, *7* (15), 6943−6951.
(64) Cao, L.-X.; Shen, Y.; Zhang, K.; Su, Z.-H.; Feng, S.-C.; Hu, X.-M.; Zhang, Y.-H.; Wang, B.-F.; Li, Y.-Y.; Gao, X.; Wang, W.-J.; Kera, S.; Ueno, N.; Li, Y.-Q.; Tang, J.-X. In Situ Interface Reaction Enables Efficient Deep-Blue Perovskite Light-Emitting Diodes. *Angew. Chem., Int. Ed.* **2025**, *64* (39), No. e202513617.
(65) Dong, J.; Lu, F.; Wang, J.; Zhang, Y.; Ma, X.; Zhou, J.; Han, D.; Zang, Z.; Wang, N. Perovskite Light-Emitting Diodes with Low Roll-off Efficiency via Interfacial Ionic Immobilization. *Chemical Engineering Journal* **2022**, *429*, 132347.
(66) Liu, X.-K.; Xu, W.; Bai, S.; Jin, Y.; Wang, J.; Friend, R. H.; Gao, F. Metal Halide Perovskites for Light-Emitting Diodes. *Nat. Mater.* **2021**, *20* (1), 10−21.
(67) Kumawat, N. K.; Liu, X.-K.; Kabra, D.; Gao, F. Blue Perovskite Light-Emitting Diodes: Progress, Challenges and Future Directions. *Nanoscale* **2019**, *11* (5), 2109−2120.
(68) Pang, P.; Jin, G.; Liang, C.; Wang, B.; Xiang, W.; Zhang, D.; Xu, J.; Hong, W.; Xiao, Z.; Wang, L.; Xing, G.; Chen, J.; Ma, D. Rearranging Low-Dimensional Phase Distribution of Quasi-2D Perovskites for Efficient Sky-Blue Perovskite Light-Emitting Diodes. *ACS Nano* **2020**, *14* (9), 11420−11430.
(69) Yuan, S.; Wang, Z.-K.; Xiao, L.-X.; Zhang, C.-F.; Yang, S.-Y.; Chen, B.-B.; Ge, H.-T.; Tian, Q.-S.; Jin, Y.; Liao, L.-S. Optimization of Low-Dimensional Components of Quasi-2D Perovskite Films for Deep-Blue Light-Emitting Diodes. *Adv. Mater.* **2019**, *31* (44), 1904319.
(70) Xue, X.; Zhao, Z.; Zhang, H.; Lin, X.; Ning, Y.; Wang, L.; Ji, W.; Zhu, H. High-Efficiency Perovskite Light-Emitting Diodes Enabled by Introducing a LiF Modification Layer. *Appl. Phys. Lett.* **2025**, *126* (1), 013501.
(71) Li, Z.; Cao, K.; Li, J.; Du, X.; Tang, Y.; Yu, B. Modification of Interface between PEDOT:PSS and Perovskite Film Inserting an Ultrathin LiF Layer for Enhancing Efficiency of Perovskite Light-Emitting Diodes. *Org. Electron.* **2020**, *81*, 105675.
(72) Shi, Y.; Wu, W.; Dong, H.; Li, G.; Xi, K.; Divitini, G.; Ran, C.; Yuan, F.; Zhang, M.; Jiao, B.; Hou, X.; Wu, Z. A Strategy for Architecture Design of Crystalline Perovskite Light-Emitting Diodes with High Performance. *Adv. Mater.* **2018**, *30* (25), 1800251.
(73) Yuan, F.; Ran, C.; Zhang, L.; Dong, H.; Jiao, B.; Hou, X.; Li, J.; Wu, Z. A Cocktail of Multiple Cations in Inorganic Halide Perovskite toward Efficient and Highly Stable Blue Light-Emitting Diodes. *ACS Energy Lett.* **2020**, *5* (4), 1062−1069.
(74) Yuan, F.; Xi, J.; Dong, H.; Xi, K.; Zhang, W.; Ran, C.; Jiao, B.; Hou, X.; Jen, A. K.-Y.; Wu, Z. All-Inorganic Hetero-Structured Cesium Tin Halide Perovskite Light-Emitting Diodes With Current Density Over 900 A Cm-2 and Its Amplified Spontaneous Emission Behaviors. *Physica status solidi (RRL) - Rapid Research Letters* **2018**, *12* (5), 1800090.
(75) Chen, Z.; Li, Z.; Chen, Z.; Xia, R.; Zou, G.; Chu, L.; Su, S.-J.; Peng, J.; Yip, H.-L.; Cao, Y. Utilization of Trapped Optical Modes for White Perovskite Light-Emitting Diodes with Efficiency over 12%. *Joule* **2021**, *5* (2), 456−466.
(76) Chen, Z.; Yuan, C.; Chen, S. Micrometer-Scale-Thick Quantum-Dot LEDs with Notably Enhanced Stability and Ultrahigh Brightness. *Science Advances* **2025**, *11* (26), eads7770.
(77) Lee, S. I.; Liang, K.; Hui, L. S.; Arbi, R.; Munir, M.; Lee, S. J.; Kim, J. W.; Kim, K. J.; Kim, W. Y.; Turak, A. Necessity of Submonolayer LiF Anode Interlayers for Improved Device Performance in Blue Phosphorescent OLEDs. *Journal of Materials Science: Materials in Electronics* **2021**, *32* (1), 1161−1177.
(78) Turak, A. On the Role of LiF in Organic Optoelectronics. *Electronic Materials* **2021**, *2* (2), 198−221.
(79) Cosset, F.; Celerier, A.; Barelaud, B.; Vareille, J.-C. Thin Reactive LiF Films for Nuclear Sensors. *Thin Solid Films* **1997**, *303* (1), 191−195.
(80) Montereali, R. M.; Almaviva, S.; Bonfigli, F.; Cricenti, A.; Faenov, A.; Flora, F.; Gaudio, P.; Lai, A.; Martellucci, S.; Nichelatti, E.; Pikuz, T.; Reale, L.; Richetta, M.; Vincenti, M. A. Lithium Fluoride Thin-Film Detectors for Soft X-Ray Imaging at High Spatial Resolution. *Nuclear Instruments and Methods in Physics Research Section A: Accelerators, Spectrometers, Detectors and Associated Equipment* **2010**, *623* (2), 758−762.
(81) Nadeau, J. S.; Johnston, W. G. Hardening of Lithium Fluoride Crystals by Irradiation. *J. Appl. Phys.* **1961**, *32* (12), 2563−2565.

Downloaded from pubs.acs.org/aaembp/article-pdf/8/4/1456/6315247/ei5c02309.pdf by SOUTHWEST JIAOTONG UNIV user on 07 November 2026

https://doi.org/10.1021/acsaelm.5c02309
ACS Appl. Electron. Mater. 2026, 8, 1456−1465